A Disorder-Aware Multi-fidelity Framework for Robust Prediction of Superconducting Critical Temperature

Nam Hai Le [1,2] **Tri Minh Nguyen** [1] **Linh La** [1] **Sherif Abdulkader Tawfik** [1] **Truyen Tran** [1]

[1]*Applied Artificial Intelligence Initiative, Deakin University* [2]*School of Information Technology, Deakin University*. Correspondence to: Tri Minh Nguyen tri.nguyen1@deakin.edu.au.

1. Introduction

Superconductivity enables lossless current transport and high-field electromagnetic devices [1, 2], but discovering high-T_c materials remains challenging [3]. While machine learning offers a promising shortcut by learning structure–property relations from large databases, two practical bottlenecks limit predictive accuracy for T_c. First, experimental crystal structures frequently exhibit disorder, where a crystallographic site may contain multiple chemical species (substitutional disorder) or multiple displaced instances (positional disorder). Second, high-fidelity 3D crystal structures with experimentally measured T_c are scarce; meanwhile, low-fidelity structure proxies can be obtained cheaply (e.g., composition-matched approximations) but are noisier.

Prior disordered-crystal models (e.g., SODNet) handle substitutional disorder by linearly combining elemental embeddings according to occupancies, effectively collapsing a multi-instance site into a single averaged representation [4]. This can obscure disorder effects and reduce robustness, especially on the disorder-only subset where correct modeling of local environments is crucial [4]. In parallel, multi-fidelity learning has improved materials property prediction by combining small high-fidelity datasets with larger low-fidelity ones, but the approach must carefully account for reliability gaps between fidelities [5, 6, 7].

We propose FiDeTGraph, combining (i) explicit disorder modeling via virtual nodes and (ii) fidelity-aware training via a graph-level fidelity embedding, yielding improved and robust T_c prediction under disorder and data scarcity.

2. Methods

2.1 Virtual-node representation for disordered sites

We convert a periodic crystal into a graph whose nodes are atomic sites and edges connect near neighbors within a cutoff. For CIFs containing disordered sites, we parse each raw disordered cluster and split it into single-atom instances $\{S_{c,k}\}$ (one per distinct species instance or displaced position). We then add one auxiliary virtual node v_c located at the cluster centroid and connect v_c bidirectionally to all $S_{c,k}$. This avoids occupancy-weighted collapse and allows v_c to summarize higher-order disorder context through message passing.

Two modalities. *Substitutional disorder (SD):* multiple species share the same coordinate with fractional occupancies; we create one instance per species and connect them to v_c. *Positional disorder (PD):* the same species appears at multiple displaced coordinates with partial occupancies; we keep all displaced instances and connect them to v_c at the centroid. Illustration is provided in Fig. 1.

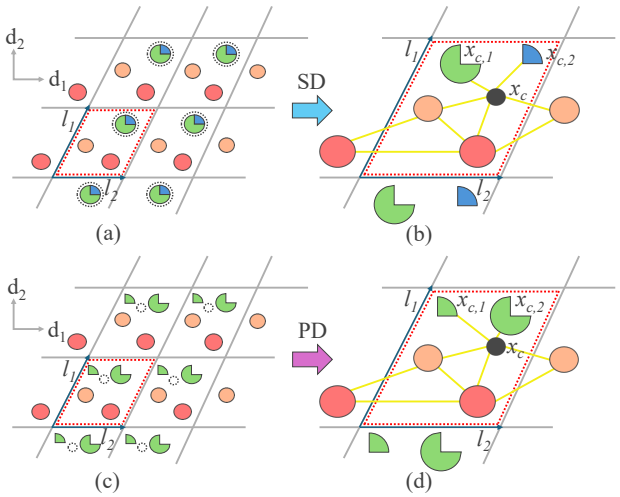

Fig. 1: Illustration of the periodic pattern of disordered crystals. Dotted red lines mark the minimum repeat cells, while grey lines indicate one possible unit cell tiled to form the infinite crystal. Dotted black circles denote virtual node placements, and yellow lines represent atomic connections in the crystal graph. (a)→(b): Transformation of a substitutionally disordered 2D crystal. Each multi-atom substitutional site is split into single-atom sites at the same fractional coordinate, with a virtual node bidirectionally connected to all atoms in the cluster ($x_c = x_{c,k},\ k \in K_c$, where K_c is the set of atoms at that site). (c)→(d): Transformation of a positionally disordered 2D crystal. Positional disorder introduces shifts breaking atomic symmetry. In the graph, a virtual node is placed at the centroid of each positional cluster and linked bidirectionally to its atoms ($x_c = \frac{1}{K_c}\sum_{k=1}^{K_c} x_{c,k}$, where K_c is the set of atoms in the cluster).

2.2 Multi-fidelity data and supercell-permuted augmentation

We use SuperCon3D as high-fidelity data (experimentally curated 3D structures with measured T_c) [4]. As low-fidelity data, we use 3DSCMP, a composition-matched dataset built from Materials Project structures with approximations when exact matches are not available, and include non-superconductors [8, 9]. To increase structural diversity aligned with disorder, we generate 2×2×2 supercells and sample multiple supercell-permuted variants by converting fractional

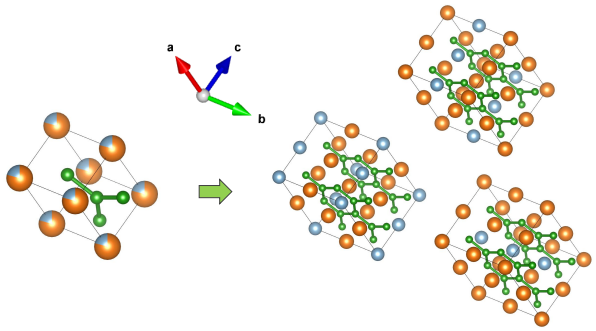

Fig. 2: Illustration of generating three distinct supercell-permuted variants of a crystal structure.

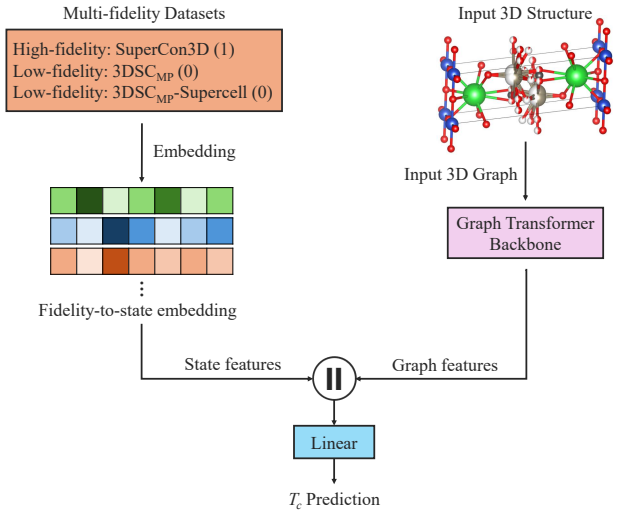

Fig. 3: FiDeTGraph architecture. Each crystal is converted to a 3D graph and encoded by an SE(3)-equivariant graph transformer to obtain graph features. A fidelity label indexes a learnable fidelity embedding, which is concatenated (||) with graph features and fed to a linear head to predict T_c.

occupancies into discrete assignments while preserving global stoichiometry, as illustrated in Fig. 2. These variants provide implicit augmentation and controlled structural uncertainty.

2.3 *FiDeTGraph: SE(3) graph transformer with fidelity embedding*

As illustrated in Fig. 3, FiDeTGraph processes the virtual-node crystal graph using an SE(3)-equivariant graph transformer backbone [10], producing node embeddings that are pooled into a graph representation h_g. Each sample also carries a discrete fidelity label f_g (e.g., SuperCon3D vs. 3DSCMP vs. 3DSCMP-supercell), mapped by a trainable embedding lookup $W_F(f_g)$. We concatenate h_g with $W_F(f_g)$ and predict T_c:

$$\hat{y}_g = \phi(h_g \,\|\, W_F(f_g)).$$

The fidelity embedding lets the model adapt its prediction to data reliability, exploiting low-fidelity coverage while anchoring to high-fidelity supervision.

Table 1: Comparison of model performance on the SuperCon3D dataset, evaluated using mean absolute error (MAE) and coefficient of determination (R^2) in log K. Results are reported for both the full dataset (order + disorder) and the disorder-only subset.

Method	MAE (logK)	R^2 (logK)
SuperCon3D: disorder subset		
XGB-Magpie	0.586 ± 0.066	0.673 ± 0.087
XGB-Magpie+DSOAP	0.577 ± 0.066	0.688 ± 0.083
iComformer	0.683 ± 0.080	0.544 ± 0.194
SODNet	0.551 ± 0.081	0.608 ± 0.224
SODNetV	0.513 ± 0.077	0.695 ± 0.135
FiDeTGraph	**0.414 ± 0.043**	**0.795 ± 0.086**
SuperCon3D: full dataset		
XGB-Magpie	0.706 ± 0.040	0.688 ± 0.050
XGB-Magpie+DSOAP	0.707 ± 0.041	**0.692 ± 0.048**
iComformer	0.750 ± 0.052	0.572 ± 0.061
SODNet	0.709 ± 0.064	0.614 ± 0.067
SODNetV	0.674 ± 0.066	0.637 ± 0.072
FiDeTGraph	**0.598 ± 0.049**	0.685 ± 0.062

3. Result

Table 1 compares FiDeTGraph with baselines on SuperCon3D [4] for both the full dataset and the disorder subset. We also report SODNetV, which integrates our virtual-node representation into SODNet [4], to isolate the benefit over occupancy-weighted averaging. Results are shown as mean±std for MAE and R^2.

Crystal representation improvement with SODNetV. On the disorder subset, SODNetV reduces MAE from 0.551 to 0.513 and increases R^2 from 0.608 to 0.695, showing that explicit disorder clusters preserve information lost by occupancy-weighted collapse.

Feature representation improvement with FiDeTGraph. FiDeTGraph improves MAE to 0.414 and R^2 to 0.795 on the disorder subset, and also improves on the full dataset. This suggests fidelity-aware training can leverage broad low-fidelity coverage while learning to discount its noise [5, 6, 7].

4. Conclusion

We introduce FiDeTGraph, a disorder-aware multi-fidelity framework for robust T_c prediction from 3D crystal structures. FiDeTGraph (i) models disordered sites via virtual nodes and (ii) integrates heterogeneous data using a graph-level fidelity embedding within an SE(3)-equivariant graph transformer. On SuperCon3D, it consistently outperforms strong baselines on both the disorder-only subset and the full dataset. Future work will study uncertainty calibration across fidelities, finer-grained fidelity modeling, and scaling to broader materials families for large-scale screening, with principled high-throughput evaluation and ablations under varying disorder levels.

References

[1] A. I. Braginski. Superconductor electronics: Status and outlook. *Journal of Superconductivity and Novel Magnetism*, 32(1):23–44, 2019.

[2] J. L. MacManus-Driscoll and S. C. Wimbush. Processing and application of high-temperature superconducting coated conductors. *Nature Reviews Materials*, 6(7):587–604, 2021.

[3] Sarah Lee. The quantum leap: Superconductivity explained. `https://www.numberanalytics.com/blog/superconductivity-explained-quantum-computing`, June 2025. Number Analytics Blog.

[4] Pin Chen, Luoxuan Peng, Rui Jiao, Qing Mo, WANG Zhen, Wenbing Huang, Yang Liu, and Yutong Lu. Learning superconductivity from ordered and disordered material structures. In *The Thirty-eight Conference on Neural Information Processing Systems Datasets and Benchmarks Track*, 2024.

[5] Chi Chen, Benjamín Sánchez-Lengeling, Jon Paul Janet, Wengong Jin, Jianyi Yang, Bradley Kimbal, Erlend A. H. Hansen, Kan Chen, Jianwei Ma, Hanchen Wang, Alex H. Lee, Shuichi H. San, Krishna Sridhar, Howard Chang, Hao Yan, Srikanth Balachandran, Robert M. Smith, Bradley D. Sherrill, Peiran Wei, Dylan J. Garvin, Ethan H. Chiang, Andrew E. Cohen, and Tobias M. Stokes. Learning properties of ordered and disordered materials from multi-fidelity data. *Nature Computational Science*, 1(1):46–53, 2021.

[6] G. Pilania, J. E. Gubernatis, and T. Lookman. Multi-fidelity machine learning models for accurate bandgap predictions of solids. *Computational Materials Science*, 129:156–163, 2017.

[7] Abhirup Patra, Rohit Batra, Anand Chandrasekaran, Chiho Kim, Tran Doan Huan, and Rampi Ramprasad. A multi-fidelity information-fusion approach to machine learn and predict polymer bandgap. *Computational Materials Science*, 172:109286, 2020.

[8] Timo Sommer, Roland Willa, Jörg Schmalian, and Pascal Friederich. 3DSC– a dataset of superconductors including crystal structures. *Scientific Data*, 10(1):1–13, Nov 2023.

[9] Anubhav Jain, Shyue Ping Ong, Geoffroy Hautier, Wei Chen, William Davidson Richards, Stephen Dacek, Shreyas Cholia, Dan Gunter, David Skinner, Gerbrand Ceder, and Kristin A. Persson. Commentary: The materials project: A materials genome approach to accelerating materials innovation. *APL Materials*, 1(1):011002, 2013.

[10] Keqiang Yan, Yuzhou Liu, Yu Lin, and Shuiwang Ji. Complete and efficient graph transformers for crystal material property prediction. In *Proceedings of the International Conference on Learning Representations (ICLR)*, 2024.